A simulation model for acid sulphate soils, I: basic principles

J.J.B. Bronswijk and J.E. Groenenberg

DLO – Winand Staring Centre for Integrated Land, Soil and Water Research (SC-DLO),
P.O. Box 125, 6700 AC Wageningen, The Netherlands

Abstract

A computer Simulation Model for Acid Sulphate Soils (SMASS) has been developed to predict effects of water management strategies, such as drainage or leaching, on acidification and de-acidification, and on release and movement of elements in including toxid elements acid sulphate soils.

SMASS consists of:
- A water transport sub-model;
- A pyrite oxidation and oxygen transport sub-model;
- A solute transport sub-model;
- A chemical sub-model.

The output consists of the soil water balance, the oxygen concentrations in the soil air, the solute concentration in the soil solution, and the amount of minerals, including pyrite, in the soil. Time steps for model simulations are in the order of hours. The output of SMASS and its sub-models is generally given on a daily basis. Model predictions can be done over periods of decades, so that long-term effects of various water management strategies can be predicted quantitatively.

Introduction

Adequate soil and water management is essential for sustainable agriculture in acid sulphate soil areas. Development of optimum water management strategies for new land reclamation projects, or for rehabilitation of existing projects, in coastal plains with acid sulphate soils requires knowledge about future consequences of the various possible water management options. Both the consequences for the soil quality in situ, i.e. inside the reclaimed areas, and downstream of the reclamation project (e.g. coastal mangrove forests) should be considered.

In acid sulphate soils, numerous complex physical and chemical processes determine the magnitude and rate of acidification and production of toxic compounds. Furthermore, chemical processes in acid sulphate soils may continue for a long time. For example, complete oxidation of all pyrite present in a soil may take decades. Long-term prediction of these complex chemical processes and their practical consequences is only feasible by using simulation models. Development of such models was recommended repeatedly (Dost and van Breemen 1982, Dent 1986, Dost 1988).

The objective of our study was to develop a computer simulation model, which can predict effects of water management strategies, such as drainage and irrigation, on acidification and de-acidification of acid sulphate soils under various conditions of soil and climate. To obtain such a model, a joint Indonesian/Dutch research project was set-up in Southern Kalimantan, Indonesia. Over a period of three years, extensive laboratory and field experiments for model development and validation have been conducted (AARD/LAWOO 1992). The resulting model combines physical processes such as transport of oxygen, water and solutes, and chemical processes such as oxidation/reduction, complexation, adsorption/desorption and precipitation/dissolution of chemical compounds. The model output includes the acidity and the chemical quality (toxicity) of soil, groundwater and drainage water. The model facilitates the evaluation of various water management strategies for land reclamation or project rehabilitation.

This article summarizes the basic principles of the model. A second article (Van Wijk et al. 1993) describes its validation and application.

General model principles

The Simulation Model for Acid Sulphate Soils (SMASS, Figure 1) consists of a number of sub-models in which the various physical and chemical processes occurring in acid sulphate soils are described using mathematical equations. In order to solve these equations, the soil profile has to be divided into compartments which may be of variable size (Figure 2).

The initial physical and chemical conditions in each compartment must be given as model input. For the complete simulation period, values for the boundary condi-

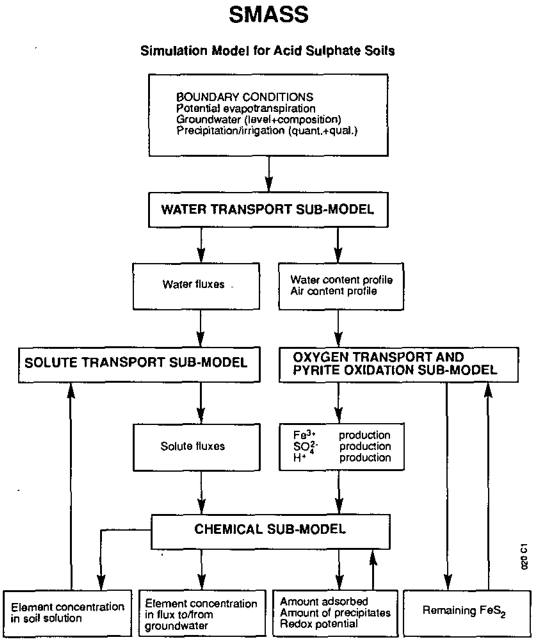

Figure 1 The structure of the model

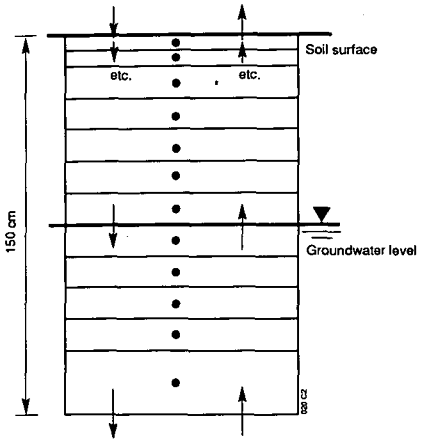

Figure 2 Schematization of a soil profile, as applied in the SMASS model. Arrows indicate water and solute fluxes

tions, as given in Figure 1, are required as input as well. The physical and chemical conditions in each compartment, together with the water and solute fluxes at the boundary of the soil system are computed at selected time intervals.

Figure 1 illustrates the sequence in which the various physical and chemical processes are computed within each time-step:

1) The *water transport sub-model* computes vertical water transport. This yields the water content profile in the soil and, as a corollary, the air content;
2) In the *oxygen transport and pyrite oxidation sub-model*, air contents are used to compute oxygen diffusion coefficients in the air-filled soil macropores. Oxygen consumption values in the soil are calculated from pyrite and organic matter contents. Subsequently, the oxygen content profile in the soil macropores is computed;
3) Depending on the oxygen concentration in a given compartment, the rate of pyrite oxidation in that compartment is now calculated in the *oxygen transport and pyrite oxidation sub-model*. The amount of pyrite it is converted into amounts of H^+, Fe^{3+} and SO_4^{2-} produced for each compartment. The amount of pyrite remaining in the soil is used for calculations in the next time step;
4) The *solute transport sub-model* computes solute fluxes between soil compartments, depending on the calculated water fluxes (step 1);
5) In the *chemical sub-model*, first the production/consumption terms for the non-equilibrium processes (such as iron reduction) are calculated. Then the total concentrations of each chemical component are calculated in the soil compartments by summing, for each component, the production/consumption terms, the inflow/outflow (from step 4), and the total amounts from the previous time-step. From these total concentrations, the equilibrium concentrations in the soil solution, the composition of the exchange complex, and the amount of minerals and precipitates are computed for each compartment.

Time steps for computations of the water and solute transport sub-models are in the order of hours. Pyrite oxidation, oxygen profiles and chemical equilibria are computed once for every day. The output of the model and its sub-models is generally given on a daily basis. If desired, each sub-model can be applied independently. Water transport can be simulated and validated first, for instance, before computing the chemical reactions. Model predictions can be carried out for one or more decades, so that the long-term effects of various water management strategies can be evaluated quantitatively.

Solute transport and chemical processes have been modelled independently: one step to solve the transport equations and a second step to solve the equations defining the chemical composition of the system.

Water transport sub-model

Schematization and modelling

The water transport sub-model is based on the SWATRE model (Feddes et al. 1978, Belmans et al. 1983). SWATRE calculates one-dimensional vertical transient water flow in soils. The basic flow equation of SWATRE is

$$\frac{\partial h}{\partial t} = \frac{1}{C(h)} \frac{\partial}{\partial z}\left[K(h)\left(\frac{\partial h}{\partial z} + 1\right)\right] - \frac{S(h)}{C(h)} \qquad (1)$$

in which

h = soil water pressure head (cm)
t = time (d)
$C(h)$ = differential moisture capacity $d\Theta/dh$ (cm^{-1})
z = vertical coordinate (positive upwards) (cm)
$K(h)$ = hydraulic conductivity ($cm\ d^{-1}$)
$S(h)$ = water uptake by roots (d^{-1})

Solving Equation 1 yields the flux of water through the upper and lower boundary of each soil compartment (Figure 2). For the top and bottom compartments, boundary conditions determine the flux at the upper and lower boundary of the soil profile. The complete set of equations is solved by an implicit finite difference scheme, applying a Thomas algorithm.

With respect to the boundary conditions at the top (precipitation/irrigation, evaporation, evapotranspiration) and the bottom of the soil system (groundwater level, pressure heads, free drainage, fluxes) various options are possible, which make the model flexible and generally applicable.

Input parameters and output

The required input parameters for the water transport sub-model are hydraulic functions of each soil horizon, boundary condition values (e.g. precipitation, potential evapotranspiration, groundwater level, flux-groundwater level relation) and crop parameters in the case of cropped soils. The output of the water transport sub-model consists of daily values of the water balance terms of the soil profile such as actual evaporation, flux through the soil surface and through the bottom of the soil profile, water flow between the various soil compartments, and water contents and pressure heads of each soil compartment.

Solute transport sub-model

Schematization and modelling

To model solute transport, the existing SWASALT model (Kroes 1991) has been extended for transport of more than one chemical component and for transport in the saturated zone. For the solute transport module, the soil profile has been divided into the same compartments that have been used in the water transport sub-model. Within these compartments complete mixing of the solutes has been assumed. For each compartment a mass conservation equation is formulated according to

$$V(n,t)\,\frac{dC(n,t)}{dt} + C(n,t)\,\frac{dV(n,t)}{dt} + q_{out} \cdot C_{out}(n,t) = q_{in} \cdot C_{in}(n,t) \qquad (2)$$

in which

$C(n,t)$ = concentration of a solute in layer n at time t (mol cm^{-1})
$V(n,t)$ = volume of water in layer n at time t (cm)
q_{in} = incoming flux in layer n (cm d^{-1})
q_{out} = outgoing flux from layer n (cm d^{-1})
C_{in} = concentration of incoming flux (mol cm^{-1})
C_{out} = concentration of outgoing flux (mol cm^{-1})

The incoming fluxes and concentrations of layer n which are the outgoing fluxes and concentrations of the adjacent layer n-1 or n+1, depending on the direction of flow, have been assumed to be constant within one time step. The mean concentration of the adjacent compartment over the time step has been used for the concentration of the incoming flux. Since the calculations are done in the direction of flow, the concentration of the incoming flux is known. Assuming constant flow rates within one time step, the change in water contents will be linear with time

$$\frac{d\Theta}{dt} = \frac{\Theta(t) - \Theta(t-1)}{\Delta t} = a \qquad (3)$$

Θ = water content ($m^3\ m^{-3}$)
a = differential water content (d^{-1})

The conservation equation can be rewritten as

$$\frac{dC(n,t)}{dt} + a \cdot \frac{q_{out}}{L(\Theta(t-1) + a \cdot \Delta t)} * C\,(n,t) = \frac{q_{in} \cdot C_{in}}{L(\Theta(t-1) + a \cdot \Delta t)} \qquad (4)$$

in which:

L = thickness of the compartment (cm)

Solutions for equation 4 for different conditions are given in Berghuijs-van Dijk et al. (1985).

Input parameters and output

The required input data for the solute transport sub-model are initial concentrations of the solutes in the soil profile, concentrations of solutes in irrigation water, precipitation and groundwater, depending on the used boundary conditions and water fluxes between the compartments (output from the water transport sub-model).

The output of the solute transport sub-model consists of the incoming and outgoing flux of elements for the various soil compartments.

Oxygen transport and pyrite oxidation sub-model

Schematization

Oxygen plays a central role in the chemical processes occurring in acid sulphate soils. The concentration of oxygen at a certain depth in the soil determines the rate of pyrite oxidation at that depth (Dent and Raiswell 1982). The principles of the oxygen transport and pyrite oxidation sub-model have been outlined by Bronswijk et al. (1993). For steady-state conditions, the gaseous oxygen concentration profile in the air-filled pores of the soil is described by (e.g. Christensen et al. 1986)

$$\frac{\partial}{\partial x}\left(D_s(\varepsilon_g)\frac{\partial C_a(x)}{\partial x}\right) = \alpha_v \qquad (5)$$

in which:

$C_a(x)$ = concentration of oxygen in air-filled pores (m^3 oxygen m^{-3} air)
$D_s(\varepsilon_g)$ = diffusion coefficient of oxygen in air-filled pores ($m^2\,d^{-1}$)
x = distance (m)
α_v = volumetric oxygen consumption rate in the soil (m^3 oxygen per m^3 soil per day)
ε_g = air-filled porosity

To solve this equation, the oxygen consumption term α must be quantified. A thin section (30-40 cm depth) of an acid sulphate soil from Barambai, Indonesia is pictured in Figure 3a. At the same depth, sites can be distinguished where pyrite is still present

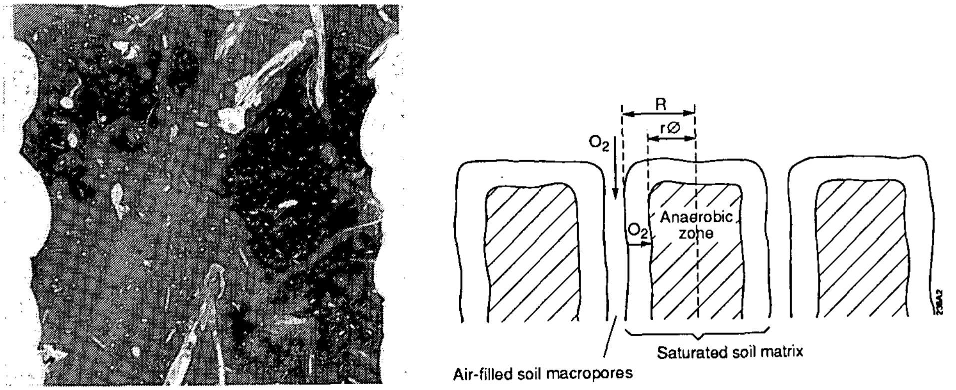

Figure 3 Two-dimensional distribution of oxygen in a structured acid sulphate soil

a. Thin section Barambai (30-40 cm depth). Pyrite is still present in the dark zones. In the grey zones all pyrite has been oxidized.

b. Model representation. R = radius of the soil aggregates (m), r = thickness of the anaerobic zone (m) and sites where pyrite has been disappeared. The grey zones in Figure 3a, containing no pyrite, are relatively close to air-filled macropores. From these macropores oxygen has been diffused into the soil matrix, whereby pyrite has oxidized. The black zones, which still contain pyrite, are further from the macropores so that oxygen has not yet penetrated.

Figure 3b shows the schematization of such a structured acid sulphate soil, as applied in the model. In SMASS, an acid sulphate soil is considered as a configuration of relatively large, partly air-filled macropores, such as shrinkage cracks, and a wet soil matrix. In heavy clay soils, the soil matrix in between the macropores will remain saturated throughout the year (Bronswijk and Evers-Vermeer 1990).

In the model approach as pictured in Figure 3b, two main processes were distinguished: lateral diffusion of dissolved oxygen from the macropores into the saturated soil matrix and vertical diffusion of gaseous oxygen through the air-filled macropores. The two processes interact at the walls of the macropores where gaseous oxygen dissolves into the soil solution of the matrix. The equilibrium between dissolved and gaseous oxygen at the walls of the macropores has been described in our sub- model by Henry's law: $[O_2]_{air} = K_H * [O_2]_{water}$, in which K_H is Henry's constant. This constant is temperature dependent. At 20 °C, $K_H = 29.7$; at 30 °C, $K_H = 52$.

Modelling of diffusion of dissolved oxygen into the soil matrix

Oxygen is mainly consumed by two processes inside the soil matrix: decomposition of organic matter and oxidation of pyrite. Because oxygen consumption by organic matter decomposition is largely independent of local oxygen concentrations (e.g. Christensen et al. 1986), the oxygen consumption rate by organic matter decomposition (α^{om}) is described in the model by

$$\begin{aligned} \alpha^{om} &= Q, \text{ for } C_w > 0 \\ \alpha^{om} &= 0, \text{ for } C_w = 0 \end{aligned} \tag{6}$$

with Q being a constant (kg O_2 m^{-3} soil day^{-1}); C_w = local dissolved oxygen concentration (kg O_2 m^{-3} water).

Disappearance of pyrite crystals by oxidation is modelled by combining the equal diameter reduction model (Swartzendruber and Barber 1965) with the McKibben and Barnes rate expression for pyrite oxidation (McKibben and Barnes 1986). This yields

$$\frac{dm}{dt} = \frac{-0.311262\sqrt{C_w}}{\rho d} X_{FeS_2} \tag{7}$$

in which:

dm/dt = rate of disappearance of pyrite crystals (kg d^{-1} m^{-3} soil)
X_{FeS_2} = pyrite content (kg per m^3 soil)
ρ = density of pyrite (kg.m^{-3})
d = average diameter of pyrite crystals (m)

Pyrite oxidation has been described in our sub-model by the chemical reaction equation

$$FeS_2 + 3\tfrac{3}{4}O_2 + \tfrac{1}{2}H_2O \rightarrow Fe^{3+} + 2\,SO_4^{2-} + H^+ \tag{8}$$

According to Equation 8, one kg of pyrite consumes one kg of oxygen. Therefore, Equation 7 also offers a quantitative expression for the mass oxygen consumption by pyrite oxidation inside the soil matrix, α_m. The steady-state equation for the dissolved oxygen concentration profile inside the soil matrix then reads

$$D_w \frac{d^2C_w(x)}{dx^2} = \alpha_m \tag{9}$$

in which:

D_w = diffusion coefficient of oxygen in the soil solution ($m^2\ d^{-1}$)

The oxygen consumption term α_m on the right hand side of this equation is equal to dm/dt from Equation 7.

Solving Equation 9 yields the dissolved oxygen concentration profile, $C_w(x)$ (kg O_2 m^{-3}) and the thickness of the aerobic zone inside the soil matrix (m). Furthermore, the total oxygen consumption β_m (kg oxygen m^{-3} soil per day) is computed by integrating $\alpha_m(x)$ over the thickness of the aerobic zone. This yields

$$\beta_m = \frac{A'C_b + Q'}{-\sqrt{B}} \left(\frac{1 - e^{2\sqrt{B}(R - r\phi)}}{1 + e^{2\sqrt{B}(R - r\phi)}} \right) . O \tag{10}$$

in which:

B = A'/D_w
A' and Q' = parameters in the linear approximation of the relationship between oxygen consumption and oxygen concentration: $\alpha_m = A'C_w + Q'$
C_b = dissolved oxygen concentration at the boundary between soil matrix and macropores (kg O_2 m^{-3} water)
O = the surface area of the soil matrix in one m^3 of soil (m^{-1})
R = radius of the soil aggregates (m)
$r\phi$ = thickness of the anaerobic zone (m)

The oxygen consumption by organic matter within one m^3 of soil is equal to

$$\beta_m^{o.m.} = \frac{Q\,(R - r\phi)}{R} \tag{11}$$

and the oxygen consumption by pyrite equals

$$\beta_m^{FeS_2} = \beta_m - \beta_m^{o.m.} \tag{12}$$

Modelling of vertical diffusion of gaseous oxygen through the air-filled macropores

Equation 5 describes steady-state gaseous oxygen profiles in the soil macropores. After conversion into volumetric units, β_m from Equation 12 is equal to α_v in Equation 5. The relation between diffusion coefficient, D_s ($m^2\ d^{-1}$), and air content, ε_g ($m^3\ m^{-3}$), is described in the model by (Bronswijk 1991):

$$D_s(\varepsilon_g) = F(1 - (1 - \varepsilon_g)^{2/3})D_o \tag{13}$$

in which:

D_o = diffusion coefficient of oxygen in the atmosphere ($m^2\ d^{-1}$)
F = empirical tortuosity factor (–)

From the oxygen consumed by pyrite (Equation 12) we can calculate the amount of oxidized pyrite (Equation 8). This yields the production of Fe^{3+}, H^+, and SO_4^{2-}. Because the oxygen consumption rate depends on the oxygen concentration (Equation 7) and, reversely, the oxygen concentration depends on the oxygen consumption rate (Equation 5), an iterative procedure has been applied in the oxygen transport sub-model to solve Equation 5 (Berghuijs-Van Dijk et al. 1985).

Input parameters and output

The required input parameters for the oxygen transport and pyrite oxidation sub-model are:

- Average diameter of structural elements;
- Air content profile (output of water transport sub-model);
- Initial pyrite content and organic matter content;
- Initial average diameter of the pyrite crystals;
- Tortuosity factor.

The output of the sub-model consists of:

- Oxygen distribution in the soil macropores and matrix;
- Produced H^+, Fe^{3+}, SO_4^{2-} (input for chemical sub-model);
- Remaining FeS_2.

A typical example of a simulated oxygen distribution is presented in Figure 4.

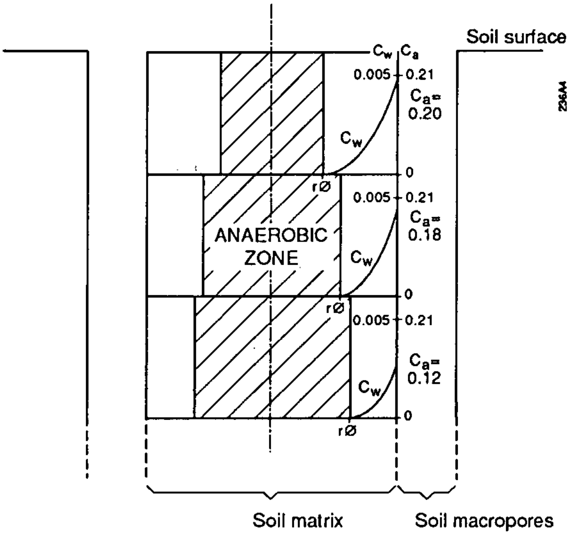

Figure 4 Example of a simulated two dimensional steady-state oxygen concentration profile in a structured acid sulphate soil. C_w = oxygen concentration in water (kg O_2 m^{-3} water), C_a = concentration of oxygen in air-filled macropores (m^3 O_2 m^{-3} air), $r\phi$ = thickness of the anaerobic zone (m)

Chemical sub-model

Schematization

All important chemical processes for acidification and deacidification are incorporated in the model SMASS. Furthermore, processes which determine the concentrations of the toxic elements Fe^{2+},Al^{3+} and of the basic cations Mg^{2+},K^+ and Ca^{2+} in the soil solution are included. Table 1 gives an overview of the most important processes.

In the chemical sub-model, the same division of the soil in compartments has been used as in the other sub-models (Figure 2). Each soil compartment consists of a mineral phase, a cation exchanger phase and a solution phase.

Within each compartment, the solution is assumed to be completely mixed with uniform concentrations.The chemical sub-model computes, for each time step, the changes in chemical composition of each compartment. First, production and consumption due to oxidation and reduction processes is calculated. These data, together with data on the inflow and outflow of solutes from/to neighbouring compartments, and data taken from the previous time step on (i) the total quantity of adsorbed cations and (ii) mineral precipitates present will result in new total amounts for each compartment. From these total amounts, ion association, cation exchange and weathering/ precipitation are calculated. This results in new concentrations of the soil solution, amounts of cations adsorbed and amounts of minerals for each compartment.

In order to describe the chemistry, a set of independent chemical components is chosen such that all the chemical species considered can be built up from this set. The components used within SMASS are: H^+, Na^+, Ca^{2+}, Mg^{2+}, Fe^{2+}, Al^{3+}, SO_4^{2-}, HCO_3^-, Cl^-, e^- (electron) and X^- (adsorption site). For the complete set of species see AARD/LAWOO 1992.

Oxidation processes

Pyrite oxidation has been described under Modelling of diffusion of dissolved oxygen into the matrix. Oxidation of adsorbed Fe^{2+}, which is much faster than the oxidation of aqueous iron (Ahmad and Nye 1990), in depyritized top layers can be a source of acidification. However, in the soils of Pulau Petak there is hardly any adsorbed Fe^{2+} in the oxidized non-pyritic top layers as a result of leaching (AARD/LAWOO 1992). This is expected to be the same in other acid sulphate soils in the humid tropics. In pyritic layers, adsorbed iron (II) can compete with pyrite for the available oxygen but pyrite oxidation is considered to be the dominant process. Therefore, oxidation of Fe^{2+} has not yet been included in SMASS, but could be important for soils in other regions.

Reduction processes

Because the concentrations of NO_3^- in acid sulphate soils are negligible and amounts of Mn(III/IV)-oxides are generally very low the most likely electron acceptor is Fe^{3+}. Reduction of $Fe(OH)_3$ is given by

$$Fe(OH)_3 + \frac{1}{4}CH_2O + 2H^+ \rightarrow Fe^{2+} + \frac{1}{4}CO_2 + \frac{11}{4}H_2O \tag{14}$$

in which $Fe(OH)_3$ represents any reducable ferric oxide and CH_2O schematically represents organic matter. Because iron contents of oxidized topsoil layers in Pulau Petak

Table 1 Chemical processes and their effects in acid sulphate soils. Processes included in SMASS are indicated.

Process	Effects	Included in SMASS
Rate-limited Processes		
Pyrite oxidation	Acidification, produces Fe^{3+} and SO_4^{2-}	yes
Iron oxidation	Acidification, lowers Fe^{2+} concentration	no
Iron reduction	Deacidification, raises concentration of Fe^{2+}	yes
Sulphate reduction	Deacidification, raises sulphide concentration	no
Weathering of primary minerals	Produces basic cations, consumes protons	no
Weathering of secondary minerals/precipitates	Consumes protons, regulates Fe^{2+} and Al^{3+} concentrations	yes
Instantaneous Processes		
Cation exchange	Buffers pH and determines concentrations of Ca^{2+} and Mg^{2+}	yes
Ion association	Raises equilibrium concentrations, especially of Al^{3+}	yes

are generally low, iron reduction mainly occurs in recently oxidized pyritic layers that have undergone submergence again.

Reduction of sulphate may also occur. However at pH below 5 sulphate-reducing bacteria are inhibited and, also, the reduction of ferric oxides inhibits or prevents sulphate reduction. Therefore, sulphate reduction has not been incorporated into SMASS.

In SMASS, iron reduction starts when a soil layer is saturated with water. The model distinguishes two forms of Fe(III)-oxides: reducable ferric oxide and non-reducible ferric oxide. The transformation of reducible iron (III) into non-reducible iron (III) is described according to

$$\Delta[Fe(OH)_3^R] = -k_1(pH)\,[Fe(OH)_3^R] \cdot \Delta t \qquad (15)$$

in which:

$[Fe(OH)_3^R]$ = the amount of reducable $Fe(OH)_3$ ($mol.kg^{-1}$)

$k_1(pH)$ = rate constant (h^{-1}).

Reduction of reducable ferric oxide is described by:

$$\Delta[Fe(OH)_3^R] = -k_2 \cdot \Delta t \qquad (16)$$

in which:

k_2 = rate constant ($mol.kg^{-1}.h^{-1}$)

New amounts of reducable iron (III) oxide are calculated by combining Equations 15 and 16 and adding the amount of precipitated $Fe(OH)_3$ calculated in the precipitation/dissolution subroutine. From the amount of oxide reduced and the stoichiometry of Equation 14, the produced amounts of Fe^{2+}, OH^- and HCO_3^- are calculated.

Ion association

In acid sulphate soils, total concentrations of Al^{3+} and other cations in equilibrium with a solid phase can be raised by the complexation of these ions with anions (e.g. sulphate). Ion association has to be taken into account to calculate the activities of the chemical components since cation exchange and mineral equilibria are related to activities and not to total concentrations. Ion speciation is also of importance in relation to toxicity, as certain species of an element are more toxic than others.

Schematically, the formation of species B_j out of the components $[A_1.A_N]$ can be represented by

$$a_{1j} A_1 + \ldots\ldots + a_{ij} A_i + \ldots\ldots\ldots + a_{Nj} A_N = B_j \tag{17}$$

According to the Law of Mass Action, the concentration of each species B_j is given by

$$[B_j] = K_j \prod_{i=1}^{N} [A_i]^{a_{ij}} \tag{18}$$

in which:

K_j = the conditional equilibrium constant including activity corrections (AARD/LAWOO, 1992)

$[A_i]$ = the concentration of the free ionic component (mol l^{-1})

Weathering and dissolution of minerals

Weathering of minerals buffers the pH of the soil solution. Weathering of primary minerals such as felspars releases basic cations such as K^+, Mg^{2+} and Ca^{2+}. Because of high weathering rates in the humid tropics, soils in these areas contain little or no primary minerals. In general these soils contain mainly kaolinite. Therefore, weathering of primary minerals has not been incorporated in SMASS. Weathering of kaolinite is too slow to maintain equilibrium. Near-equilibrium concentrations of aluminium values with other aluminium bearing minerals and precipitates have been found in acid sulphate soils. In the soils of Pulau Petak, the concentrations of Al^{3+} at pH values around 5 and higher tend to equilibrium with amorphous $Al(OH)_3$. This was also found by Patrick and Moore (1991) for acid sulphate soils in Thailand. At a lower pH and high sulphate concentrations, Al^{3+} concentrations seem to be regulated by a basic aluminium sulphate, jurbanite (Nordstrom 1982). Van Breemen (1976) postulated the regulation of Al^{3+} concentrations by a basic aluminium sulphate for acid sulphate waters in Thailand based on activity calculations for Al^{3+} and SO_4^{2-} from which he found a linear relationship between $pAl(OH)_3$ and pH_2SO_4. This was also found for the soils in Pulau Petak (AARD/LAWOO 1992) and by Moore and Patrick (1991). At low pH and high SO_4^{2-} concentrations, jurbanite is more stable than gibbsite and amorphous $Al(OH)_3$. From the solubility products it can be deduced that jurbanite is stable over amorphous hydroxide below a pH_2SO_4 of 13.0 (AARD/LAWOO 1992). For activities of sulphate around 5 mmol l^{-1} jurbanite is more stable than amorphous aluminium hydroxide for pH values below 5.3, which is very general in acid sulphate soils. In the model equilibrium with jurbanite has been assumed.

The dissolution of jurbanite buffers one proton according to

$$Al(OH)SO_4 + H^+ \rightarrow Al^{3+} + SO_4^{2-} + H_2O \tag{19}$$

At pH values below 3, dissolution of iron oxides and iron hydroxides becomes important. The buffer intensity of this process depends on the solubility of the iron (hydr)oxide. From an examination of the data of the column and field experiments (AARD/LAWOO 1992) it is clear that various iron oxides determine the solubility of Fe^{3+}. In the model the solubility product of goethite has been used to calculate the iron concentration in the soil solution if ferric oxide is present.

The congruent dissolution of a solid phase B_j can be written as:

$$B_j \rightleftarrows a_{ij}A_1 + ..a_{ij}A_i.. + a_{nj}A_n \tag{20}$$

in which A_1 .. A_n are aqueous components. The concentrations of A_1 to A_n tend to equilibrium at which their activity product (Q_j) will be equal to the solubility product (K_j) of the particular precipitate. The activity product is defined as:

$$Q_j = \prod_{i=1}^{n} (A_i)^{a_{ij}} \tag{21}$$

If the rate is proportional to the difference between the activity product and the solubility product, the change in the total concentration of component A_i can be written as

$$\frac{d[A_i]^T}{dt} = \sum_{j=1}^{m} a_{ij}k_j\,[Q_j - K_j] \cdot \rho/\theta \tag{22}$$

in which:

k_i = rate constant

ρ = bulk density of the solid phase (kg m^{-3})

This equation can be approximated with finite differences according to

$$\Delta[A_i]^T = \sum_{j=1}^{m} \Delta t\, a_{ij}\, k_j\,[Q_j - K_j] \cdot \rho/\theta \tag{23}$$

Cation exchange reactions

Cation exchange can buffer the pH of the soil solution by the exchange of acidic cations such as H^+ and Al^{3+} against basic cations as Mg^{2+} and Ca^{2+}. Exchange reactions also control the concentrations of Ca^{2+} and Mg^{2+} in acid sulphate soils (Moore and Patrick 1989). Schematically, cation exchange can be written as

$$z_bA^{za+} + z_aBX_{z_b} \leftrightarrows z_aB^{zb+} + z_bAX_{z_a} \tag{24}$$

in which X denotes one adsorption site at the cation exchange complex, A and B are cations and z the valence of the cation. Cation exchange is included for Ca^{2+}, Mg^{2+}, Na^+, K^+, Al^{3+} and Fe^{2+}.

Cation exchange has been modeled with the Gaines-Thomas expression (see Bolt 1967).

$$K_{A/B} = \frac{E_A{}^{zb}\,(B^{zb+})^{za}}{E_B{}^{za}\,(A^{za+})^{zb}} \tag{25}$$

in which brackets denote activities in the solution, E stands for the equivalent fraction adsorbed, which is the amount adsorbed of a component in equivalents divided by the total adsorption capacity, and K is the exchange coefficient.

Cation exchange can be written as the sum of two half reactions which are similar to the equations for the ion association (AARD/LAWOO 1992).

Solution technique
For each component a mass balance can be formulated according to

$$[A_i]^T_{t-1} = \sum_{j=1}^{m} a_{ij}\, k_j \prod_{i=1}^{n} [A_i]^{a_{ij}} + \Delta [A_i]^T \qquad (26)$$

in which:

$[A_i]_{t-1}^T$ = the total quantity of component i in solution and adsorbed at the previous time step (mol l^{-1})

$[A_i]$ = the concentration of the free ionic component (mol l^{-1})

$\Delta\,[A_i]^T$ = the change in the total concentration of A_i due to weathering/precipitation (mol l^{-1}), see equation 22.

This formula results in a set of n equations with n unknowns which is solved with a Newton Raphson iteration scheme (Groenendijk 1993).

Input parameters and output
The required input parameters for the chemical sub-model are:

System parameters
- Thermodynamic equilibrium constants;
- Cation exchange coefficients;
- Rate constants for precipitation/dissolution and redox reactions;
- Cation exchange capacity (CEC) of each compartment;
- Dry bulk density of each compartment.

Initial conditions
- Initial pH, pE and total concentrations of the elements for each compartment;
- Initial moisture fractions;
- Initial amounts of precipitates.

Variable conditions
- pH, pE and total concentrations of the elements for rainwater, irrigation water and groundwater;
- Produced amounts of H^+, Fe^{3+} and SO_4^{2-} (from the oxygen transport and pyrite oxidation sub-model);
- Incoming amounts of the chemical elements for each layer from the solute transport sub-model

The output of the model consists of the pH, pE and total concentrations of all the chemical components for the soil solution in the various compartments and the composition of the drainage water. Further, the model gives the amounts of adsorbed cations and precipitates.

Acknowledgement

This research has been carried out as part of the 'Research Program on Acid Sulphate

Soils in the Humid Tropics', which is a collaborative Dutch-Indonesian research project, by LAWOO (Land and Water Research Group), The Netherlands, and AARD (Agency for Agricultural Research and Development) Indonesia. This research was partly sponsored by the Netherlands Directorate General of International Cooperation (DGIS).

References

AARD/LAWOO 1992. Acid sulphate soils in the humid tropics. Volume 3: Simulation model of physical and chemical processes in acid sulphate soils to evaluate water management strategies. AARD, Jakarta

Ahmad, A.R. and P.H. Nye 1990. Coupled diffusion and oxidation of ferrous iron in soils. I. Kinetics of oxygenation of ferrous iron in soil suspension. J. Soil Sci. 41: 395-409

Belmans, C, J.G. Wesseling and R.A. Feddes 1983. Simulation of the water balance of a cropped soil: SWATRE. J. Hydrol. 63: 271-286

Berghuys-van Dijk, J.T., P.E. Rijtema and C.W.J. Roest, 1985. ANIMO, agricultural nitrogen model. ICW-note 1671, Wageningen

Bolt, G.H. 1967. Cation exchange equations used in soil science. A review. Neth. J. Agric. Sci. 15: 81-103

Breemen, N. van 1976. Genesis and solution chemistry of acid sulphate soils in Thailand. Pudoc, Wageningen

Bronswijk, J.J.B. 1991. Magnitude, modeling and significance of swelling and shrinkage processes in clay soil. PhD thesis, Agricultural University Wageningen

Bronswijk, J.J.B. and J.J. Evers-Vermeer 1990. Shrinkage of dutch clay soil aggregates. Neth. J. Agric. Sci. 38: 175-194

Bronswijk, J.J.B., K. Nugroho, I.B. Aribawa, J.E. Groenenberg, C.J. Ritsema 1993. Modeling of oxygen transport and pyrite oxidation in acid sulphate soils. J. of Environmental Quality

Christensen, T.H., B.L. Parker, and J.C. Refsgaard 1986. A model for the unsaturated zone; oxygen transport and consumption model. Report Danish Hydraulic Institute. Horsholm

Dent, D.L. 1986. Acid sulphate soils: a baseline for research and development. ILRI Publ. 39. International Institute for Land Reclamation and Improvement, Wageningen

Dost, H. (editor) 1988. Selected papers of the Dakar symposium on acid sulphate soils. ILRI Publ. 44, International Institute for Land Reclamation and Improvement, Wageningen

Dost, H. and N. van Breemen 1982. Proceedings of the Bangkok Symposium on Acid Sulphate Soils, January 1981. ILRI Publ. 31, International Institute for Land reclamation and Improvement, Wageningen

Feddes, R.A., P.J. Kowalik, and H. Zaradny 1978. Simulation of field water use and crop yield. Pudoc, Wageningen

Groenendijk, P. 1993. The calculation of complexation, adsorption, ion exchange, precipitation and weathering reactions in a soil-water system with the geochemical model EPIDIM. Staring Centre Report 70, DLO Winand Staring Centre, Wageningen

Kroes, J.G. 1991. Transol 2.1, A dynamic model for transport and transformation of solutes in soils. User's guide. Internal report 110, DLO Winand Staring Centre, Wageningen

McKibben, M.A., and H.L. Barnes 1986. Oxidation of pyrite in low-temperature acidic solutions: rate laws and surface textures. Geochimica et Cosmochimica Acta. Vol. 50: 1509-1520

Moore, P.A. and W.H. Patrick Jr. 1989. Calcium and magnesium availability and uptake by rice in acid sulfate soils. Soil Sci. Soc. Am. J. 53: 816-822

Moore, P.A. Jr. and W.H. Patrick Jr. 1991. Aluminium, boron and molybdenum availability and uptake by rice in acid sulfate soils. Plant and Soil 136: 171-181

Nordstrom, D.K. 1982. The effect of sulfate on aluminum concentrations in natural waters: some stability relations in the system Al2O3-SO3-H2O at 298 K. Geochim. Cosmochim. Acta 46: 681-692

Ritsema, C.J. Estimation of activity coefficients of individual ions in solution with ionic strengths up to 0.3 mol l^{-1}. Submitted to J. Soil Sci.

Swartzendruber and Barber, 1965. Dissolution of limestone particles in soil. Soil Sc. 100: 287-291

Wijk, A.L.M. van, I. Putu Gedjer Widjaja-Adhi, C.J. Ritsema and C.J.M. Konsten 1993. A simulation model for acid sulphate soils, II: Validation and Application. In: D.L. Dent and M.E.F. van Mensvoort (editors) Selected papers of the Ho Chi Minh City symposium on acid sulphate soils. Publication 53, 357-367 International Institute for Land Reclamation and Improvement, Wageningen

A simulation model for acid sulphate soils, II: Validation and application

A.L.M. van Wijk[1], I Putu Gedjer Widjaja-Adhi[2], C.J. Ritsema[1] and C.J.M. Konsten[1]

[1] The Winand Staring Centre for Integrated Land, Soil and Water Research, P.O. Box 125, 6700 AC Wageningen, The Netherlands
[2] Centre for Soil and Agroclimate Research, Bogor, Indonesia

Abstract

The Simulation Model for Acid Sulphate Soils (SMASS) was validated by comparing model predictions with measurements obtained during extensive laboratory and field experiments in acid sulphate soils from Southern Kalimantan, Indonesia. Using the model, pH and concentrations of major ions such as Al^{3+}, Mg^{2+} and SO_4^{2-} in the soil solution could be predicted at various depths for both actual and potential acid sulphate soils. Different water management strategies such as drainage, submergence and leaching were considered for both fresh and brackish water conditions. Subsequently, SMASS has been applied to evaluate various possible water management strategies for acid sulphate soils in the same area. It was shown that for an actual acid sulphate soil located in a backswamp with rainwater conservation and tidal drainage, that continuation of the current water management combined with leaching with good quality water could considerably reduce soil acidity. Moderate drainage at 40 cm depth and leaching with water of improved quality (to pH = ±5) at the end of the wet season was found as a favourable water management option to improve an ill-drained potential acid sulphate soil with pyrite starting at 15 cm, also located in the same backswamp area. After 3 to 4 years the upper 35 cm is free of pyrite and subsequently shows a fast reduction of acidity and Al^{3+} concentrations.

SMASS can predict the long-term physical and chemical consequences of various water management strategies in areas with acid sulphate soils. The present water management practice in a certain area and possible alternatives can be evaluated with respect to their effects on soil and water quality.

Introduction

Simulation models that integrate main physical and chemical processes in a coherent system have been recommended as tools to evaluate water management in areas with acid sulphate soils (Dost and van Breemen 1982, Dent 1986). Therefore, the Simulation Model for Acid Sulphate Soils (SMASS) was developed to assist the selection of promising water management options. The principles of SMASS have been described by Bronswijk and Groenenberg (1993).

The present paper deals with the validation of the model and illustrates its capability for evaluating different water management strategies. Data required for the model validation were obtained from experiments with undisturbed acid sulphate soil columns from and monitored field plots in the Pulau Petak area of Southern Kalimantan, Indonesia. Also, the soil and water management options used in the model application were from Pulau Petak. A detailed description of the study area is given by Kselik et al. (1993).

Model validation

SMASS was validated by comparing model calculations with results from experiments with undisturbed soil columns subjected to controlled drainage, irrigation and leaching. In addition, model calculations have been compared with measurements from monitoring field plots located on both potential and actual acid sulphate soils in the different tidal land classes of Pulau Petak.

Column experiments

Materials and methods

Experiments with seven undisturbed soil columns of 1 m length and 25 cm diameter were carried out to study basic physical and chemical processes and to collect data for model calibration and validation. Four columns contained sulphidic clay soils and three columns ripe acid sulphate soils. The columns were subjected to the following hydrological conditions:

- Drainage to study oxidation of pyrite and subsequent acidification;
- Submerging/flooding to study reduction processes;
- Leaching with fresh and brackish water to study the removal of acidity and chemical compounds.

Every fortnight over two years, the complete water balance, oxygen concentration, redox potential, chemical composition of soil moisture at five depths and element concentrations in drainage and ponding water were measured. In addition, the initial and final hydraulic characteristics, texture, contents of organic matter, pyrite and $CaCO_3$ were measured. Four out of the seven columns, here indicated as the columns 1 to 4, were used for validation of the model. Columns 1 and 2 contained sulphidic (potentially acid sulphate) soil with pyrite from the soil surface downwards; while columns 3 and 4 were initially acid in the top (40 cm) and pyritic below. From day 1 until day 450, columns 1, 2 and 3 were subjected to drainage, keeping the groundwater table at 80 cm depth. During this period regular small irrigations with fresh (column 1) and brackish (columns 2 and 3) water were given to compensate for water losses by evaporation from the top and by soil moisture sampling. After day 450 the soil was submerged for one month with fresh (column 1) and brackish (columns 2 and 3) water. From day 480 onwards the columns were continuously leached with fresh (column 1) and brackish (columns 2 and 3) water, applying rates of 1 mm d^{-1} until day 500, 6 mm d^{-1} between days 500 and 715 and 6 mm d^{-1} from day 715 until 770.

Column 4 was subjected to fresh water submergence from day 1 until 480. After day 480, the soil was leached with fresh water with the same leaching rates as the other columns.

The model simulation was carried out over the same time span applying the same drainage, submergence and leaching/irrigation regimes as in the column experiment. The daily measured actual evaporation of the columns was given as top boundary condition in the model validation. This evaporation ranged from 1 to 1.7 mm d^{-1}. Furthermore, daily quantity and quality of irrigation water were used as top boundary condition. The daily groundwater level inside the column was given as bottom boundary condition together with the groundwater quality.

Various physical and chemical input parameters were available to run the model. An overview of the parameters needed, determination methods and values applied have been presented in AARD/LAWOO (1992a).

Results

During the validation some problems were encountered. First, due to drying of the upper layers of the columns during the drainage phase, it was not always possible to extract enough soil solution from the porous cups to carry out a complete chemical analysis. In that case, the pH was estimated with indicator paper which yielded only a very rough indication. Although great care was taken with the samples, a continuous series of measurements of high quality cannot be guaranteed. Especially pH, SO_4^{2-} and Al^{3+} were sensitive to erroneous measurements (Harmsen 1989, Supardi Suping 1990). Sometimes measured pH values of reduced bottom layers were low due to oxidation of Fe^{2+} in the sampling bottles. Samples with high ionic strength sometimes exhibit great differences between sum of cations and sum of anions; sum of anions often exceeds sum of cations, sometimes with a few hundred percent. SO_4^{2-} concentrations seemed to be too high, and aluminum too low (Supardi Suping 1990).

Figure 1 summarizes the results of the model validation. All data available on pH, Al^{3+}, Mg^{2+} and SO_4^{2-} from the four columns have been plotted against values computed for corresponding days using SMASS. Calculated and measured pH agree reasonably well within the range pH 2.5 to 7. The scattering of pH-values is obviously increased by the unreliable pH-paper measurements (which can be recognized as vertical columns of symbols at pH 3, 3.5, 4.5 and 5). Measured and calculated Al^{3+} concentrations exhibit more variability. Apart from uncertainties in measured data, other reasons may be:

- A relatively slight difference in measured and calculated pH results in a much more pronounced difference between measured and calculated Al^{3+} concentrations;
- In the model calculations, only the jurbanite equilibrium is assumed to take place while, in reality, Al-hydroxides are becoming important above pH 5;
- Constant exchange coefficients are used in the model simulations, sometimes leading to poor agreement between predicted and measured values, in particular during leaching.

The measured and predicted Mg^{2+} concentrations also indicate some dispersion. The main reason may be that the soil in the model is assumes uniform leaching, not accounting for macropore flow, leading to an overestimation of leaching efficiency. Measured and predicted SO_4^{2-} concentrations show a high similarity.

In conclusion, in spite of some noise, the relationship between the measured and computed major elements can be described by a 1:1 line over a very wide range of concentrations.

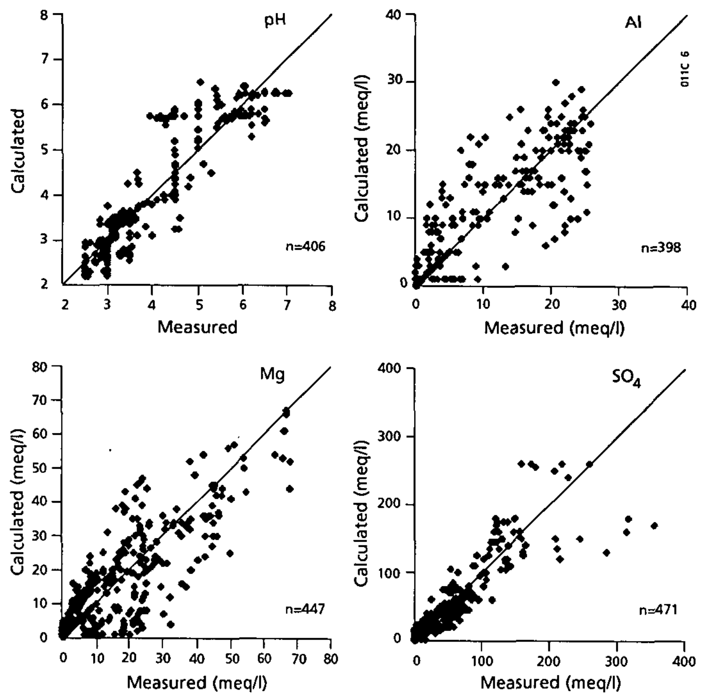

Figure 1 Comparison of model simulations of pH, Al^{3+}, Mg^{2+} and SO_4^{2-} concentrations with data measured at depths of 5, 45 and 85 cm in four columns with two undisturbed acid sulphate soils subjected to drainage, submergence and leaching with fresh or brackish water

Field experiments

Materials and methods

Conditions in the soil columns differ considerably from those in the field. Owing to rather extreme water management practices applied, the concentrations of some major elements (Al^{3+}, Mg^{2+}, SO_4^{2-}) were much higher in the columns than in the monitoring field plots.

To investigate the capability of the model under normal field conditions, SMASS was also validated by comparing model calculations with two year measurements (November 1988 to December 1990) from field plots on Pulau Petak. Five monitoring field plots were used, two on potential and three on actual acid sulphate soils. The plots were in four different tidal land classes. The following data were collected every fortnight: groundwater table depth, oxygen concentration, redox potential, chemical composition of soil solution at six depths and element concentrations in drainage and ponding water. In addition, the initial soil texture, hydraulic characteristics and contents of organic matter, pyrite, $CaCO_3$ were determined.

The validation of the model using measurements of each of these five plots has been described in AARD/LAWOO (1992a). Here, only the validation by the field plot at Tabunganen will be presented. Tabunganen is located in the coastal plain close to the sea. The soil is potential acid sulphate, with pyrite up to the soil surface, used for growing rice. The land is flooded daily with brackish water. Only during the dry period (two to three months a year), the groundwater table drops below the soil surface with a maximum depth of 15-20 cm below surface.

Groundwater levels measured at the field plot were used as the bottom boundary condition. The daily flooding regime and precipitation measured at the site were used as the top boundary condition. During flooding, brackish water of the same quality as measured in the nearby tertiary canal is infiltrating through the top boundary of the model with a rate of 10 mm d^{-1}. Potential evapotranspiration was obtained from open pan evaporation measurements and were completed with estimates from Doorenbos and Pruitt (1977) for missing periods.

Ionic concentrations, pH and redox potentials measured at the start of the monitoring period were used as initial condition for the different model compartments. Measured values of the cation-exchange capacity at different depths were used for model input. Other required input parameters and their values used have been given in AARD/LAWOO (1992a).

Results

Because groundwater levels at Tabunganen were high throughout the year, all chemical processes in Tabunganen occur in the upper 30 cm. Therefore, only the field observations and model computations for 5 and 25 cm depth will be presented.

SMASS computed the oxidation of pyrite upon aeration of the soil during the dry period in the first year of field measurements. The computed drop in pH around day 250 (Figure 2), and the corresponding rise in Al^{3+} and SO_4^{2-} concentrations, agreed with the field measurements. The leaching process in the successive wet period (starting around day 350) was shown by both computed and observed pH rise and decrease of SO_4^{2-} concentration. The model predicted aeration and pyrite oxidation in the dry period of the second year, starting around day 580 by a drop in pH, at 5 cm depth, and rise in SO_4^{2-} concentration.

In the second dry period, the model predicted a rise in SO_4^{2-} concentrations at 25 cm depth due to leaching of compounds out of the topsoil. In reality, however, concentrations at 25 cm depth were much more stable. Part of the SO_4^{2-} produced in the topsoil was, possibly, leached horizontally into the field ditches. As a result, the subsoil received less compounds from the topsoil than was computed with the one-dimensional model.

In general, however, there was a good agreement between modelled and actual conditions.

Model application to evaluate water management strategies

The model has been applied to predict the long-term effects of different water management strategies on soil properties and soil and drainage water quality for two acid sulphate soils in Pulau Petak, namely an actual acid sulphate soil (Barambai I) and a potential acid sulphate soil (Barambai II). Both soils are monitoring fields used for model validation (AARD/LAWOO 1992a).

Simulations were carried out for a period of ten years starting at the beginning of the field experiments (November 1988). To achieve a period of ten years, rainfall

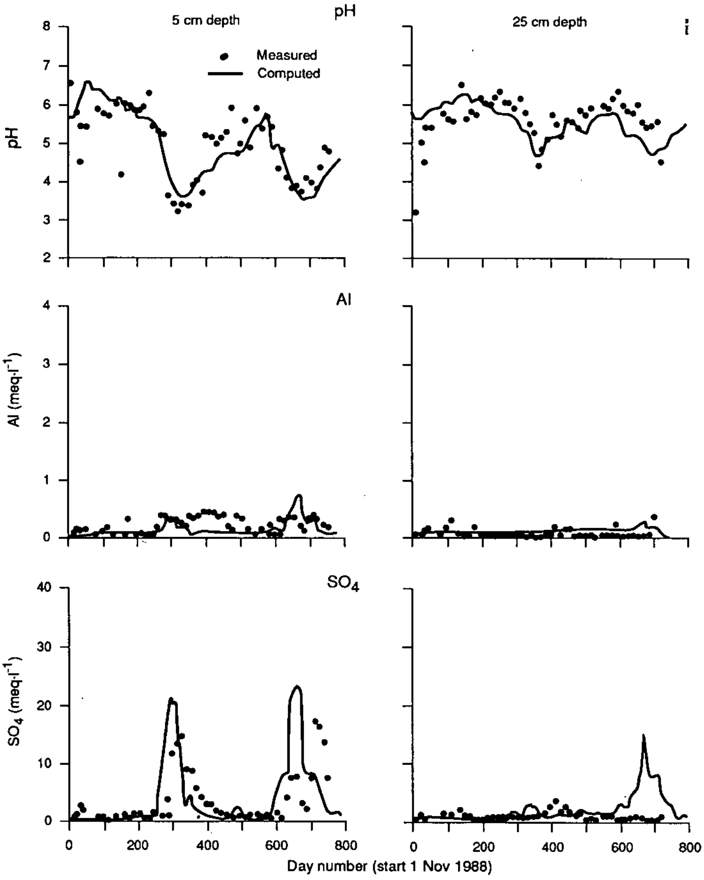

Figure 2 Comparison of simulations at pH, Al^{3+} and SO_4^{2-} concentrations at 5 cm (left-hand side) and 25 cm (right-hand side) depth with data obtained from field measurements of a potential acid sulphate soil (Tabunganen) subjected to daily flooding with brackish water

and groundwater level data collected in the period November 1988 to December 1990 were repeated five times because of lack of long-term daily weather records. Initial soil properties and other input parameters were similar to those used in the model validation.

Barambai I

Barambai I has actual acid sulphate soils (Sulfic Fluvaquents) with pyrite starting at 65 cm depth, used for growing rice. The site is located in a backswamp area in tidal land class C (Kselik et al. 1993). The current water management consists of tidal drainage and rainwater conservation. During the wet period the field is flooded for about four months. During the dry period the groundwater table falls to a maximum depth of 75 cm. Two water management strategies have been projected over ten years:

- Present water management;
- Present water management, extended with leaching in the wet season with irrigation water of good quality.

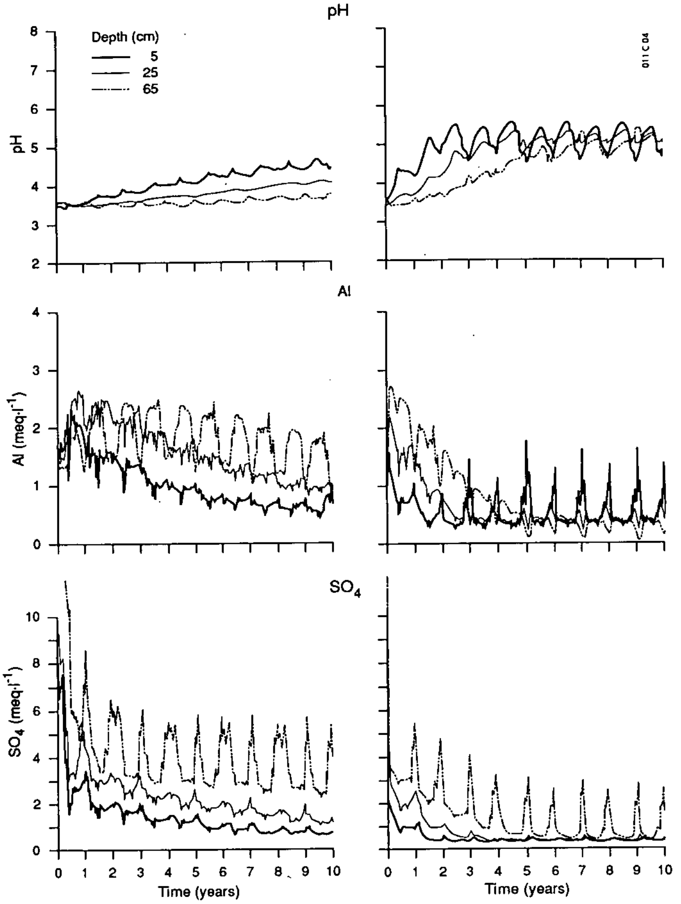

Figure 3 Model prediction of pH, Al^{3+} and SO_4^{2-} concentrations at depths of 5, 25 and 65 cm in an actual acid sulphate soil (Barambai I) for a period of ten years:
Lefthand side: present water management
Righthand side: present water management, extended with leaching with water of good quality during the wet season

Present water management

Continuation of the present water management system, with lowest groundwater levels around 75 cm depth, will not cause much pyrite oxidation because the pyritic layer starts at about the same depth (Figure 3, lefthand side). The fluctuations in pH, Al^{3+} and SO_4^{2-} are caused by dilution and leaching due to the seasonal influence of dry and wet periods. Acidity in the topsoil will be leached by rainwater, which can be seen from the very slow rise of the pH and decreasing concentrations of Al^{3+} and SO_4^{2-}. This slow improvement is only due to rainwater leaching, so continuation of the present water management does not lead to a rapid improvement of the soil.

Present water management and leaching with water of good quality

To improve an already acidified soil, the acidity must be removed. Simulations were done to evaluate the effect of leaching with water of good quality. Therefore, the soil was irrigated during the wet seasons (November to March, 30 mmd^{-1}, pH 5) over the 10 yearperiod considered. Figure 3 (righthand side) shows an increasing of pH within five years to values around 5. Also Al^{3+} and SO_4^{2-} concentrations will decrease due to the additional irrigation with good quality water.

Barambai II

Barambai II has potential acid sulphate soils (Typic Sulfaquents) with pyrite starting at 15 cm depth, used for rice cultivation. The experiment site is located within tidal land class C in the same backswamp area as Barambai I but it is outside the major influence of the drainage system. The present water management consists of rainwater conservation and restricted drainage. During the wet period the experiment site is flooded during six to seven months. The lowest groundwater levels in the dry period are around 60 cm, clearly below the pyritic layer, but reaches this depth for only 1-2 months. Besides, oxidation has only started recently, so Barambai II is in an initial stage of pyrite oxidation.

Two water management strategies have been projected over ten years:
- Continuation of the present water management;
- Drainage by keeping the groundwater level at 40 cm during the whole year to accelerate pyrite oxidation in the top 40 cm, combined with leaching with good quality irrigation water. At present this water is already available in the tertiary canals at the end of the wet season (March to May).

Present water management

Every dry season, the pH will to drop rapidly and Al^{3+}-concentrations will rise due to in situ pyrite oxidation (Figure 4, left-hand side). The reverse trend will occur in the wet season as a result of leaching and reduction. After ten years, the pyrite content of the soil profile is still high from a depth of 25 cm downwards, while soil conditions remain bad.

Combined drainage and leaching with water of good quality water

To remove pyrite from the topsoil, the effects of drainage throughout the year combined with additional leaching at the end of the wet season with good quality water from the tertiary canals have been studied.

At the end of the dry season (September to October), water in the tertiary canals has a very bad quality (pH between 2.5 and 3.5) and is not suitable for leaching purposes. At the end of the wet season (March to May), water quality in the tertiary canals is improving rapidly to pH values of around 5. Therefore, in the combined drainage – leaching scenario, irrigation was only applied during the period between March and May (30 mm d^{-1}).

Figure 4 shows that, initially, pyrite oxidation will accelerate by increased drainage giving rise to low pH and high Al^{3+} concentrations during the dry season. Leaching with good water in the following wet season improves the soil conditions considerably. The main objective of this scenario is fast removal of pyrite from the topsoil. After about three years, all the pyrite in the topsoil has been oxidized. Influenced by leaching with water of relatively good quality, soil conditions (pH, Al^{3+}) will begin to improve,

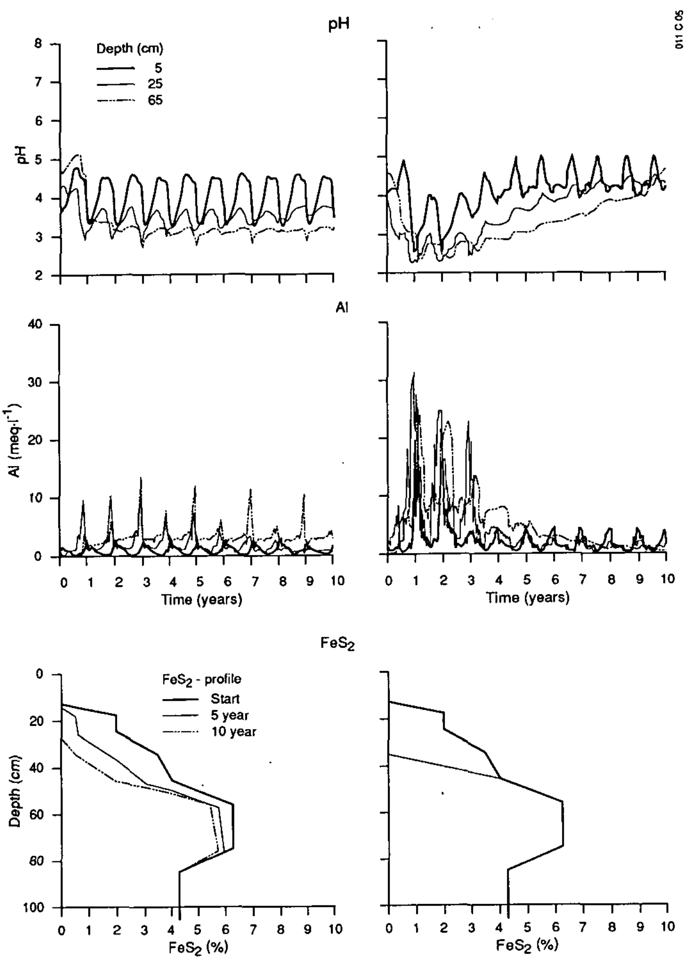

Figure 4 Model prediction of pH, Al^{3+} and SO_4^{2-} concentrations at depths of 5, 25 and 65 cm and resulting pyrite profiles (below) in a potential acid sulphate soil (Barambai II) for a period of ten years:
Left hand side: present water management
Right-hand side: drainage at 40 cm depth combined with leaching with water of good quality at the end of the wet season

because the pyrite has disappeared from the aerated zone. At the end of the period considered, the pH in the soil profile will be higher than when continuing the present water management. Moreover, the risk of acidification will be much smaller due to lowering of the top of the pyritic layer from 15 to about 40 cm below soil surface.

Conclusions

Using the SMASS model, pH and concentrations of major ions in the soil solution could be predicted at various depths for both actual and potential acid sulphate soils. Different water management strategies such as drainage, submergence and leaching for both fresh and brackish water conditions were applied.

The validation of the model by comparison of model calculations with measurements from column experiments and field plots showed a reasonably good agreement between measured and predicted pH, Al^{3+}, Mg^{2+} and SO_4^{2-} concentrations. Comparison of measured and predicted major ions yields a 1:1 relationship over a very wide range of concentrations. The greatest variability was found for Al^{3+} and Mg^{2+}, which can be ascribed partly to erroneous measurements and partly to some shortcomings of the model, related to our assumptions about leaching. The pyrite oxidation could be predicted. Resulting pH-decrease and rise in Al^{3+} and SO_4^{2-} were reasonably well predicted. SMASS offers the possibility of predicting the long-term physical and chemical consequences of various water management strategies in areas with acid sulphate soils. Present water management practices in a certain area and possible other strategies can be evaluated with respect to their effects on soil and water quality.

In the evaluation presented, the consequences of various water management strategies are predicted without discussing their implementation in practice. Implementation of promising water management strategies must be subsequently assessed by a technical and economic evaluation.

Acknowledgement

This research has been done as part of the 'Research Program on Acid Sulphate Soils in the Humid Tropics', which is a collaborative Dutch-Indonesian research project by LAWOO (Land and Water Research Group), The Netherlands, and AARD (Agency for Agricultural Research and Development), Indonesia. This research was partly sponsored by the Netherlands Directorate General for International Cooperation (DGIS).

References

AARD & LAWOO 1992a. Acid sulphate soils in the humid tropics. Volume 3: Simulation model of physical and chemical processes in acid sulphate soils to evaluate water management strategies. AARD, Jakarta

AARD & LAWOO 1992b. Acid sulphate soils in the humid tropics. Volume 4: Water management and soil fertility research in acid sulphate soils in Kalimantan, Indonesia. AARD, Jakarta

Bronswijk, J.J.B. and J.E. Groenenberg 1993. SMASS: a simulation model for acid sulphate soils, I: Basic principles. In: D.L. Dent & M.E.F. van Mensvoort (editors): Selected papers of the Ho Chi Minh City Symposium on acid sulphate soils. Publ. 53, 341-355, International Institute for Land Reclamation and Improvement, Wageningen

Dent, D. 1986. Acid sulphate soils: a baseline for research and development. ILRI Publ. 39. International Institute for Land Reclamation and Improvement, Wageningen

Doorenbos, J. and W.O. Pruitt 1977. Crop water requirements. FAO Irrigation and Drainage Paper 24. FAO, Rome

Dost, H. and N. van Breemen (editors) 1982. Proceedings of the Bangkok Symposium on Acid Sulphate Soils, January 1981. ILRI Publ. 31. International Institute for Land Reclamation and Improvement, Wageningen

Harmsen, J. 1989. Report on a mission to South-Kalimantan for quality control of chemical analyses. Mission Report 26, Research on Acid Sulphate Soils in the Humid Tropics. International Institute for Land Reclamation and Improvement, Wageningen

Hendro Prasetyo, J.A.M. Janssen, and Alkasuma 1990. Landscape and soil genesis in Pulau Petak, Indonesia. In: Papers workshop on acid sulphate soils in the humid tropics, 18-29. AARD & LAWOO, Bogor

Kselik, R.A.L., K.W. Smilde, H.P. Ritzema, Kasdi Subagyono, S. Saragih, Mauliana Damarik and H. Suwardjo 1992. Integrated research on water management, soil fertility and cropping systems on acid sulphate soils in South Kalimantan, Indonesia. In: D.L. Dent & M.E.F. van Mensvoort (editors): Selected papers of the Ho Chi Minh City Symposium on acid sulphate soils. Publ. 53, 177-194, International Institute for Land Reclamation and Improvement, Wageningen

Supardi, S. 1990. Problems of chemical analysis of water samples from acid sulphate soils. In: Papers workshop on acid sulphate soils in the humid tropics, 136-145, AARD & LAWOO, Bogor, Indonesia: 136-145